



# Evidence of preferential diffusion and segregation of impurities at grain boundaries in very pure niobium used for radiofrequency cavities

C. Antoine, B. Bonin, H. Safa, B. Berthier, E. Tessier, P. Trocelier, A. Chevarier, N. Chevarier, B. Roux

## ► To cite this version:

C. Antoine, B. Bonin, H. Safa, B. Berthier, E. Tessier, et al.. Evidence of preferential diffusion and segregation of impurities at grain boundaries in very pure niobium used for radiofrequency cavities. Journal of Applied Physics, 1997, 81, pp.1677-1682. in2p3-00007489

**HAL Id: in2p3-00007489**

**<https://hal.in2p3.fr/in2p3-00007489>**

Submitted on 26 Nov 1998

**HAL** is a multi-disciplinary open access archive for the deposit and dissemination of scientific research documents, whether they are published or not. The documents may come from teaching and research institutions in France or abroad, or from public or private research centers.

L'archive ouverte pluridisciplinaire **HAL**, est destinée au dépôt et à la diffusion de documents scientifiques de niveau recherche, publiés ou non, émanant des établissements d'enseignement et de recherche français ou étrangers, des laboratoires publics ou privés.

20

**Institut  
de Physique  
Nucléaire  
de Lyon**

Université Claude Bernard

IN2P3 - CNRS

**LYCEN 9609**  
Avril 1996

**Evidence of preferential diffusion and segregation of  
impurities at grain boundaries in very pure niobium  
used for radiofrequency cavities**

**C. Antoine, B. Bonin and H. Safa**

*CEA, DSM/DAPNIA/Service d'Etude des Accélérateurs, CE-Saclay  
F-91191 Gif-sur-Yvette, cedex*

**B. Berthier, E. Tessier and P. Trocelier**

*CEA, DSM/DRECAM/Laboratoire Pierre Süe, CE-Saclay  
F-91191 Gif-sur-Yvette cedex*

**A. Chevarier, N. Chevarier and B. Roux**

*Institut de Physique Nucléaire de Lyon, IN2P3/CNRS, Université Claude Bernard  
43 Bd du 11 Novembre 1918, F-69622 Villeurbanne cedex*

Submitted to Journal of Applied Physics

SCAN-9604178



CERN LIBRARIES, GENEVA

9609618

# **Evidence of preferential diffusion and segregation of impurities at grain boundaries in very pure niobium used for radiofrequency cavities**

C. Antoine, B. Bonin and H. Safa

*CEA, DSM/DAPNIA/Service d'Etude des Accélérateurs, CE-Saclay, 91191 Gif-sur-Yvette Cedex*

B. Berthier, E. Tessier and P. Trocelier

*CEA, DSM/DRECAM/Laboratoire Pierre Sûe, CE-Saclay, 91191 Gif-sur-Yvette Cedex*

A. Chevarier, N. Chevarier and B. Roux

*Institut de Physique Nucléaire de Lyon, IN2P3-CNRS et Université Claude Bernard, 43, Bd du 11 Novembre 1918, 69622 Villeurbanne Cedex*

## **ABSTRACT**

In order to overcome dissipation due to impurity segregation at grain boundary, niobium cavities are submitted to a purification annealing ( $1300^{\circ}\text{C} \pm 200^{\circ}\text{C}$  under vacuum) during which titanium is evaporated onto the Nb surface. The resulting titanium layer acts as a solid state getter reacting with light impurities (H, C, N, O), thereby removing these impurities from the bulk of the niobium. Evidence of preferential titanium diffusion and segregation at grain boundaries has been studied using PIXE analysis induced by proton microbeam.

(Submitted to *The Journal of Applied Physics*)

## I. INTRODUCTION

Superconducting radiofrequency cavities are a very promising technology for achieving high accelerating gradients and/or continuous beams in particle accelerators<sup>1</sup>. Different technological choices are possible among superconductors (elemental or compound, thin films or sheets ...). Nevertheless, most of the present and near future projects are based on the use of pure niobium sheets to form the cavities because the metallurgy of a pure metal is often simpler than that of compounds\*.

Although the surface resistance of a superconductor is very low, RF power is still dissipated on the surface. This is very costly in terms of cryogenic power. Over the last several years, much theoretical and experimental work has been conducted at Saclay, as well as in other laboratories, to identify and grade the different sources of power dissipation for the case of superconducting cavities made from pure niobium sheets. The influence of internal contamination<sup>2,3</sup>, trapping of magnetic flux<sup>4,5</sup>, field emission related to surface contamination<sup>6,7</sup>, and granular aspect of the polycrystalline material<sup>8,5</sup> have been explored in detail. For superconducting materials, the grain boundaries tend to be in the normal state and, therefore, act like Josephson junctions. This subject was examined in reference<sup>8</sup> for low T<sub>c</sub> superconductors. Even though these boundaries may be in the superconducting state, they might play an important role in power dissipation. The calculations show that even in the superconducting state, the resistivity of a grain boundary is related its normal-state specific resistivity. This value is very near  $10^{-16} \Omega.m^2$  for most of the very pure metals, but can be greatly influenced by impurity segregation near grain boundaries<sup>8,5</sup>.

Impurity segregation is very likely to happen in pure niobium for three reasons:

- it is very difficult to get rid of interstitials like C, N, O in BCC metals,
- impurities tend to interact with crystallographic defects<sup>21,22</sup>, and when the metal becomes very pure, the main remaining defects are interfaces like grain boundaries or free surfaces,
- evidences for surface segregation have been found<sup>2</sup>. These can be an indication of a more

---

\* *Nb is actually the pure metal with the highest transition temperature: 9.2 K*

general segregation phenomena<sup>9</sup>.

Therefore, it is very important to determine if there is impurity segregation in the niobium used to produce SC cavities, and to what extent it is responsible for the residual surface resistance. The literature points out that equilibrium segregation is often concentrated in a very few monolayers at an interface<sup>9</sup>, i.e., within  $\sim 10\text{-}15$  Å of a grain boundary. As niobium cavities generally receive several annealings, and are allowed to cool slowly under vacuum after each one, one can assume that if any segregation occurs, it will have had time to reach the equilibrium state. This could have a dramatic effect on the residual resistivity. This segregation is very difficult to detect directly because several of the analytical methods explore a volume that is huge compared to the very thin grain boundary film. Other techniques commonly used to study segregation generally are surface-sensitive techniques (e.g., ESCA). These techniques examine a freshly fractured intergranular surface. Unfortunately, in the case of niobium, fractures occur in an intragranular way<sup>10</sup>; thus, this usual techniques can not be used. Some attempts have been done to use another common technique: Transmission Electronic Microscopy, but it appeared very difficult to prepare samples in the correct state, although some evidence have been found of the existence of a secondary phase in the niobium after the same heat treatment as described here after<sup>11</sup>.

In order to overcome dissipation due to impurity segregation, Niobium cavities are generally submitted to a “purification annealing” ( $1300^{\circ}\text{C} \pm 200^{\circ}\text{C}$ , under vacuum; exact conditions depending on the laboratory), during which titanium is evaporated onto the Nb surface. The resulting titanium layer acts as a solid state getter, reacting preferentially with O, and to a lesser extent with C and N, thereby removing these impurities from the bulk of the niobium (see ref. 12 for more details on this purification phenomena). After this annealing, a chemical etching of several microns removes the surface layers of titanium, oxides and other surface contaminants. In practice, it has been observed that a low surface resistance could not be reached unless several tens of microns were removed (typically  $50\text{ }\mu\text{m}$ ). As calculations indicated that titanium would

diffuse into bulk niobium less than  $0.5\text{ }\mu\text{m}$  on average, our attention was directed to the possible presence of titanium in the grain boundaries.

For these reasons it was decided to study segregation in niobium by means of the new nuclear microprobe in the Laboratoire Pierre Süe at Saclay. This apparatus can explore very small areas (probe  $\sim 1 \times 1\text{ }\mu\text{m}^2$ , minimum). The explored depth depends strongly on the used reaction (incident energy, incident or detected particles or radiation), but a large range of nuclear reactions, and nuclear or atomic excitations are available.

Titanium can be detected with good sensitivity ( $10^{-4}/\text{At}$ ) by proton or deuteron induced X-Ray Emission (PIXE or DIXE). By using deuterium ions beam, both heavy elements and C, N, O can be profiled simultaneously by means of DIXE and nuclear reactions respectively. A simple calculation shows that a very localised concentration of titanium can be detected easily: let us suppose that there is a  $1.5\text{ }\text{\AA}$  thick layer of 100% titanium along a grain boundary, and that we choose to observe the boundary perpendicular to the sample surface (i.e., parallel to the probe beam, see Fig. 1). “Diluted” by the volume irradiated by the beam (typically a  $2\text{ }\mu\text{m}$  diameter cylinder), this leads to an effective concentration of  $\sim 10^{-4}/\text{At}$ . This indicates that segregation in quantities as low as one monolayer at a grain boundary can be detected successfully, provided that the grain orientations allow it.

In the following work, we show experimental evidence of the presence of titanium in grain boundaries of annealed and subsequently etched niobium samples. The concentration of titanium appears to depend on the relative orientation of the grains, and on the depth of a grain boundary relative to the surface of the sample.

## II. NUCLEAR MICROPROBE DESCRIPTION

It is composed of a  $3.75\text{ MV}$  Van de Graaff accelerator, equipped with a R.F. source. Three kinds of beam are currently available, protons, deuterons and  $\text{He}^4$ . Intensities of about  $50\text{ }\mu\text{A}$  are available at the output of the accelerator but they are too high to generate microbeams. We

generally use a  $5 \mu\text{A}$  beam to improve the emittance of the source by reducing the gas pressure down to  $5 \cdot 10^{-7}$  mbars. The brightness of the microbeam is typically  $100 \text{ pA}/\mu\text{m}^2$ . An analysing magnet located at 3.5 m from the exit of the accelerator ( $R = 1 \text{ m}$ ) allows to bend the beam into one of available lines. The dipole magnet is used to define the beam energy. Slits are mounted close to the image point of this magnet. The differential intensity of beam intercepted by these two slits allow to correct the High Voltage of the terminal. The observed stability may change between  $10^{-3}$  and  $5 \cdot 10^{-4}$  for energies varying between 0.3 and 3.75 MeV.

Two microbeam lines are available, they are both practically identical. They are composed of two slits systems. The first one, at the image point of the analysing magnet, defines the size of the beam at the input of the line. Its aperture is adjustable in the range  $\pm 100 \mu\text{m} \pm 0.1 \mu\text{m}$ . The second one, situated 6 m apart, defines the convergence of the beam. Its aperture is adjustable between  $\pm 5$  and  $\pm 0.1 \text{ mm}$ . These slits systems are built with stainless steel cylinders. Each couple X or Y is mounted in different plans, then each of cylinders is used partially as anti-scattering to the precedent. These slits are cooled to minimise all aperture variation during the experiments.

The beam is focused on the sample by a quadrupole doublet. The two lenses are fixed together. This mounting has been done because the poles of the lenses have been shaped all together in place. The doublet is mounted on a table to optimise the position of the optical axis with respect to the geometrical alignment. Two electrostatic deflectors are used to adjust the position of the beam on the sample. These deflectors are also used to sweep the beam on the target. The swept area can be  $1 \times 1 \text{ mm}^2$  with a minimum step of  $0.3 \mu\text{m}$  which will be reduced down to  $0.1 \mu\text{m}$  for future developments. Samples are mounted on a target holder which is fixed on a X-Y-Z- $\theta$  goniometer. The amplitude and the resolution of displacements are given in Table 1. The goniometer and the deflectors allow to adjust the beam position on the target with a higher precision than  $0.5 \mu\text{m}$ . These adjustments are perturbed from time to time by low frequency vibrations along the horizontal axis, perpendicular to the beam direction. This is

mainly induced by roughing pumps distributed along the beam lines and will be soon improved. Actually the target holder is stabilised by means of a finger fixed on the analysis chamber to avoid vibrations.

The sample and beam observation is performed with two optical microscopes. The first one has a magnification of 40. It is located at  $45^\circ$  from the beam axis and used for coarse adjustments. The second one has an annular object and allows an observation at  $0^\circ$  with a magnification of 400. These two microscopes are coupled to CCD video cameras. The lighting of the sample is insured by optical fibbers.

## **A. Experimental technique**

### **1. Detectors**

Well known analysis methods such as RBS, NRA, ERDA, PIXE, PIGE are commonly used at the microprobe. We used two type of detectors during this experiment:

- A telescope made of two silicon detectors ( $10$  or  $15\text{ }\mu\text{m}$ ,  $1500\text{ }\mu\text{m}$ ) can be positioned between  $120^\circ$  and  $150^\circ$  as an attempt to measure simultaneously Titanium and Oxygen, (not presented in this paper).
- A Si Li detector is mounted at  $150^\circ$  for X rays analysis of Titanium. Its distance to the impact point of the beam can be adjusted between  $20$  and  $80\text{ mm}$ .

### **2. Data processing**

Two kinds of data are necessary to the control the experiment: The first data set concern the beam and the target. The most important parameters are: voltages  $V_x$  and  $V_y$  applied on the electrostatic deflectors, positions  $X\ Y\ Z\ \theta$  of the target holder, integrated charge, irradiation time, conditions of sweeping (like dose per point), size of the steps, number of steps in  $X$  and  $Y$  directions. These data are processed by a PC (486). The controls have been developed with the LABVIEW<sup>13</sup> software.



The second data set concerns the studied reactions: in this case the energies measured by each detector. All these data are read by the data acquisition computer via a CAMAC transmission. A handshake take place between the PC and the CAMAC trigger during the data acquisition process. It authorises or prevents the acquisition depending on the beam or sample displacement, the dose or the irradiation time. Energies and coincidence time data are digitised and stored by CAMAC peak sensing ADC. The dose the counting rate of each detector and the irradiation time are counted by CAMAC scalers. The position parameters and  $V_y$  are stored in CAMAC registers. All these data are correlated for each event.

### **3. Sample preparation**

Samples were cut from 2 mm thick niobium sheets ( $\text{Nb} > 99,95 \text{ W\%}$ ). These sheets were also used to fabricate many of the superconducting cavities tested at Saclay in the MACSE accelerating facility<sup>14</sup>. The samples were vacuum annealed for 16 hours at  $1350^\circ\text{C}$  ( $1623\text{K}$ ) between two titanium foils. They were carefully weighed before and after this heat treatment in order to determine the thickness of the deposited titanium film (typically  $0.8 \mu\text{m}$ ). Then the samples were etched in a 1:1:2 solution of  $\text{HF}:\text{HNO}_3:\text{H}_3\text{PO}_4$  for different times in order to remove 6, 15, or  $35 \mu\text{m}$  from the surface. One drawback of this preparation technique was that it gave rise to etching features, i.e., it created a rough surface. This made it more difficult to observe and visualise the grain boundaries, but we wanted to mimic the usual surface treatment given the cavities themselves.

## **B. Experimental results**

Because of practical reasons, we made two sessions of experiments. Several grain boundaries, chosen at random on each sample, and were examined by PIXE or DIXE in the first case (PIXE), the concentration of titanium was calculated with the help of the GUPIX program, taking as an hypothesis that there was no titanium in the core of the grain (indeed, the counting was the same as on the untitanified reference samples and gave us the sensitivity threshold). In the

second case (DIXE), the concentration of titanium was calculated by comparing the counting of our samples with one from a TiN reference sample. In absolute we should also introduce in the calculations the difference of the particles penetration depth inside TiN as compared to the niobium matrix, but as the calculated concentration of titanium is only an estimation “diluted” in the explored volume, this effect is certainly second order. (Moreover, we do not know the exact local composition). We must emphasize that the concentrations showed hereafter are necessarily the lower limits of the actual local concentration.

In both experiments it quickly became evident that not all grain boundaries contained titanium. Titanium was very likely to be encountered on the 6  $\mu\text{m}$  etched sample (after a little training, we were able to predict its presence only by the visual aspect of the boundary). It was very difficult to detect on 15  $\mu\text{m}$  etched sample and not found at all on the 35  $\mu\text{m}$  sample (within the sensitivity of the microprobe). In some places where titanium was detected, the “counting” was so important that we could conclude rapidly to either an important concentration at the grain boundary, and/or a very large distribution. Table 2 shows the results of counting in the bulk grain and in the apparent grain boundary area. As a first approximation, we estimated the concentration of atomic titanium by a simple comparison with the counting of a known TiN sample. Of course these figures should be corrected, because of the particles penetration depth. But as we already have a big uncertainty about the actual local concentration of Ti due to the large explored volume, we decided for this first report to present the obtained atomic concentrations as relatives estimations. Corrected, more precise results should be published by the same authors later on, accompanied with complementary experiments<sup>15</sup>. In a same way, counting made on sample which did not undergo a titanium treatment provided us an estimation of the detection threshold (see Table 2). The concentration of titanium inside the grains was always below this threshold of the microprobe, but in grain boundaries concentrations from “0” (i.e., less than the sensitivity) to several atomic percent were found. Moreover, as can be seen in Fig. 2, the width distribution could be quite wide.

These variations, either in concentration or in width, could be influenced by three factors:

- the apparent concentration depended on the relative orientation of the adjacent grains,
- the observed grain boundary was not necessarily perpendicular to the surface. Because some depth of the sample was probed, it was difficult to send the beam exactly down the “center” of the distribution.

- the width of the titanium distribution itself might be of the same order as the beam diameter and one cannot tell if it is due to the beam or to the distribution itself.

Figure 3 shows a photographic montage of one grain boundary that was explored in detail. Note the change in concentration that occurs when the orientation of the barrier changes. This result shows that titanium can diffuse into niobium only if it finds an easy pathway. As the results in terms of concentration are diluted by the probed volume, one can expect that the segregation at the grain boundaries is locally quite large and, therefore, have a significant influence on the conducting properties of niobium.

### III. DISCUSSION

The most striking feature observed is segregation and preferential diffusion at grain boundaries.

Preferential diffusion at grain boundaries is a subject well documented in the literature<sup>9,16–22</sup> that is likely to happen in all bulk materials. Grain boundaries are the most important short circuiting path and diffusion along them is reported to be order of magnitudes (sometimes as high as  $10^6$  !) faster than through the bulk, and the activation energy for this phenomena was found considerably smaller than that of the bulk diffusion. But it is seldom possible to decouple grain boundary diffusion from volume diffusion which occur due to the leakage of the diffusant through the “walls” of the boundary into the adjoining crystal. In this case, the system may not obey the Fick’s law, the penetration depth being proportional to approximately  $t^{1/4}$  instead of  $t^{1/2}$  found for homogeneous media<sup>19</sup>.

Preferential interaction and segregation at grain boundaries is also linked to boundary free energy, which depends strongly on the orientation relationships between two adjacent grains. As those relationships depends from many parameters (five different orientation parameters, temperature, chemical state, ...) statistical studies are generally driven on the variation in only one direction, everything else being kept the same. These studies have proven that there exist some precise orientations where grain boundary energy is lower than the mean value. Moreover, regular arrays of grain boundary dislocations have now been identified in a large number of interfaces which were close to those “specific” misorientations. In many case, it has been proven that these arrays of dislocations are consistent with those to be expected in a model of “Coherent Site Lattice” interface ( the interface contains regular sets of dislocations which permit the area between them to relax to an exact misorientation, at least for low angle misorientations). In some case where “Coherent Site Lattice” cannot be applied, it seems that interfaces which can be interpreted as a plane which contains repeated groups of atoms of short period also exhibit a lower energy behaviour. At last, the average grain boundary energy is reduced, sometimes dramatically, by addition of solute<sup>18</sup>. All these considerations explain easily why preferential diffusion and segregation occur preferentially at grain boundaries, but also that it depends strongly on the orientation relationship between the adjacent grains. (This can be understood easily in terms of a “steric effect” or “free volume” left in the region adjacent to the grain frontier, although the evoked mechanism is generally vacancies migration). In metals one can summarise the main features in the following manner<sup>19</sup>:

- It is a thermally activated phenomena. The activation energy is approximately half that for volume diffusion.
- Rapid diffusion pathways are very close to the boundary itself.
- Geometrical parameters of the boundary play an important role for diffusion.
- All the experimental evidence are consistent with a mechanism based on vacancy movements.

#### IV. SUMMARY AND CONCLUSION

The presence of a noticeable concentration of titanium at a depth of several microns in niobium grain boundaries may be correlated with the high surface resistance encountered in heat treated cavities which received only a light etch. This fact is consistent with preferential diffusion and segregation of titanium along the grain boundaries. A long etch to remove deep titanium contamination from cavities is not a favourable solution because it has been demonstrated that such an etch results in hydrogen penetration of the niobium<sup>2,3</sup> this, could give rise to an increase of the surface resistance due to the existence of hydrides phases at low temperature. It seems therefore to be important to control annealing parameter very carefully and to try to minimise their number as they also deteriorate mechanical properties of the cavities.

These interesting results also encourage us in studying eventual segregation of other impurities, as we pointed out that they might be responsible for the residual resistance that still exist on niobium below 2K. Getting rid of this contamination could then give rise to a decrease of thermal dissipations, which is always appreciable in term of cryogenic power consumption ! A study about different kinds of annealings should be conducted, as their condition (annealing and cooling time, vacuum, use of different getters) can influence much eventual segregation.

## REFERENCES

- <sup>1</sup> Proceedings of the 4th Workshop on RF Superconductivity, edited by Y. Kojima, KEK, Tsukuba, Japan, Aug. 14-18, (1989).
- <sup>2</sup> B. Bonin and R. Roth, *Particles Accelerators* **40**, 59 (1992).
- <sup>3</sup> C. Antoine, Proceeding of the 5th Workshop on RF Superconductivity, DESY, p. 616, edited by D. Proch, Hamburg, Germany, August, (1991).
- <sup>4</sup> C. Vallet *et al.*, (submitted at Superconducting Science and Technology).
- <sup>5</sup> C. Vallet, PhD Thesis, Claude Bernard Lyon-1 University, (1994).
- <sup>6</sup> B. Bonin, *Field emission studies at Saclay*, Proceeding of the 6th Workshop on RF Superconductivity, p. 616, edited by R. Sundelin, CEBAF, Newport News, VA, USA, August (1993).
- <sup>7</sup> J. Tan, PhD Thesis, Paris-VI University, (1995).
- <sup>8</sup> B. Bonin and H. Safa, *Superconducting Sc. & Technol.* **4**, 257-261 (1991).
- <sup>9</sup> *Interfacial segregation*, edited by WC Johnson (1979).
- <sup>10</sup> J. F. Fries, PhD Thesis, Orsay Paris-XI University, (1972).
- <sup>11</sup> C. Z. Antoine, (1993-94 unpublished results).
- <sup>12</sup> H. Safa, D. Moffat, B. Bonin and F. Koechlin, *J. of Alloys & Compounds* **232**, 281-288 (1996).
- <sup>13</sup> National Instruments Corporation, 6504 Bridge Point Parkway, Austin, Texas, USA.
- <sup>14</sup> *MACSE*, Proceeding of the 6th Workshop on RF Superconductivity, p. 616, edited by R. Sundelin, CEBAF, Newport News, VA, USA, August (1993).
- <sup>15</sup> Same authors as this paper, (to be published).
- <sup>16</sup> E. D. Hondros and M. P. Seah, *Int. Met. Rev.*, **222**, 262-301 (1991).
- <sup>17</sup> *Diffusion in Solid Metals and Alloys*, edited by H. Mehrer, Landolt-Bornstein New Series III/26, (1991).
- <sup>18</sup> *Grain Boundary Structure and Kinetics*, edited by R. W. Balluffi, ASM Material Science Seminar Books, (1979).

- <sup>19</sup> I. Kaur and W. Gust, *Fundamentals of Grain and Interphase Boundary Diffusion*, edited by Ziegler Press, Stuttgart, (1989).
- <sup>20</sup> I. Kaur, W. Gust and L. Kozma, *Handbook of Grain and Interphase Boundary Diffusion*, edited by Ziegler Press, Stuttgart, (1989).
- <sup>21</sup> B. Roux, PhD Thesis, Claude Bernard Lyon-I University, (1993).
- <sup>22</sup> B. Roux, H. Jaffrezic, N. Chevarier and M. T. Magda, Phys. Rev. B **52**, 4162 (1995).

## TABLE CAPTIONS

**TABLE 1.** Characteristics of the goniometer.

**TABLE 2.** Counting for titanium. (a) Note that the limit of sensitivity varies slightly with the experimental session. (b)  $\langle C \rangle$  represents the overage value over all measurements of the category.



## FIGURE CAPTIONS

**FIG. 1.** Scheme describing the geometry of the analysed system in case of a  $2\text{ }\mu\text{m}$  diameter beam and a depth probe noted  $\ell$ .

**FIG. 2.** Detected concentration of titanium while crossing a grain boundary.

**FIG. 3.** Photographic montage of one grain boundary that was explored in detail. Note the change in concentration that occurs when the orientation of the barrier changes.

Axis	Amplitude (mm)	Resolution ( $\mu\text{m}$ )
X	20	0.5
Y	150	0.5
Z	20	0.5
$\theta$ (degrees)	180°	0.01°

TABLE 1.

Sample	Bulk of the grain	Boundary
no heat treatment	Ti not detected, limit of sensitivity = 200 to 500 atppm <b>(a)</b>	
heat treatment with Ti etched 6 $\mu\text{m}$	0 - 1500 atppm < C > ~ 500 atppm <b>(b)</b>	0 - 37000 atppm < C > ~ 5000 atppm <b>(b)</b>
heat treatment with Ti etched 15 $\mu\text{m}$	169 - 305 atppm < C > ~ 228 atppm <b>(b)</b>	9 - 6215 atppm < C > ~ 736 atppm <b>(b)</b>
heat treatment with Ti etched 35 $\mu\text{m}$	Ti not detected	

TABLE 2.

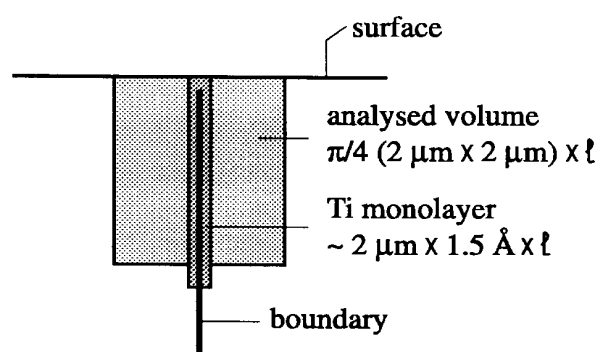


FIG. 1.

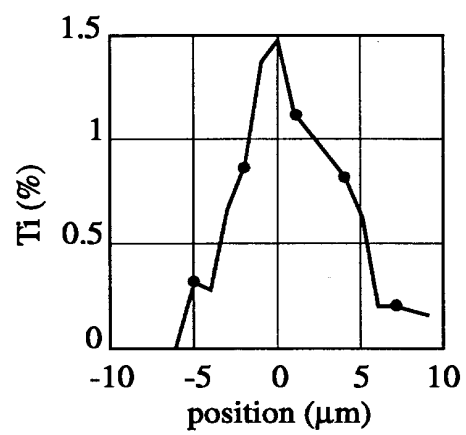
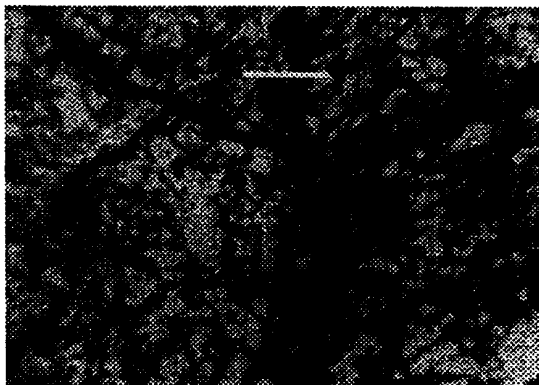


FIG. 2.

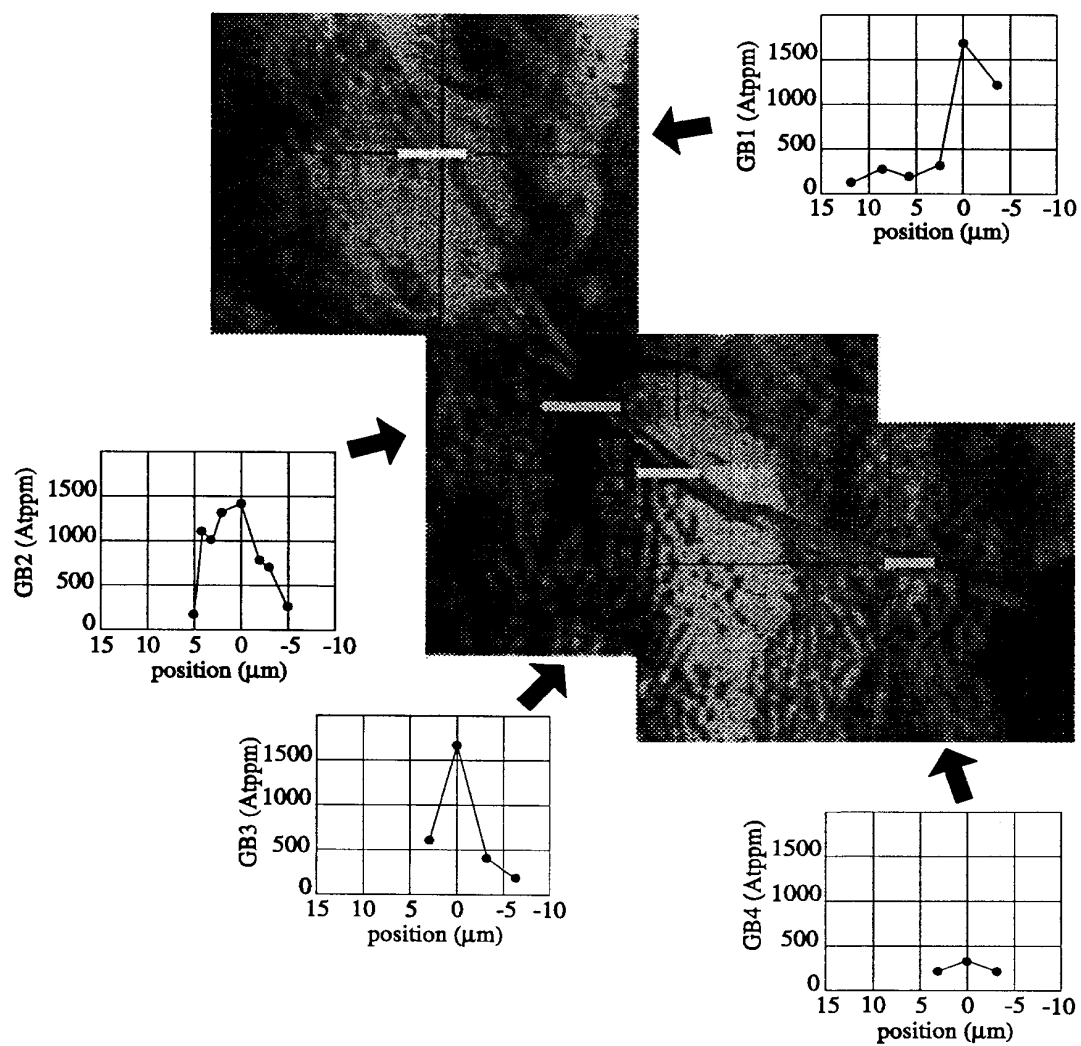


FIG. 3.